N66-147

Physical Properties of Aromatic Hydrocarbons

Part II Solidification Behaviour of 1:3:5 Tri-α-Naphthylbenzene

J. H. Magill and D. J. Plazek

Mellon Institute
4400 Fifth Avenue
Pittsburgh, Pennsylvania 15213

Presented in part at the Seventh Symposium on Polymer and Fiber Microscopy, September 1965, Textile Research Institute, Princeton, New Jersey

Abstract

The kinetics of solidification of 1:3:5 tri-α-naphthylbenzene have been studied from 25° above the glass temperature (69°C) almost to the crystal thermodynamic melting point (199°C). The crystal growth rate has been analyzed using current theories of crystallization and a mechanism for crystal growth has been proposed. It has been demonstrated that mass transport in crystal growth and viscous flow do not have the same temperature dependence. The morphology of the solid phase is discussed. Pertinent parameters pertaining to the glassy state of this material are also reported.

Introduction

Some years ago, it was demonstrated that branched hydrocarbon molecules exhibited anomalous or "excess" viscosity behaviour when compared with planar compounds of similar molecular weight.[1,2,3] It was found that the zero shear melt viscosity of these non-planar molecules could not be described by the Arrhenius equation with a single activation energy. It was also noted that the more structurally complex the material, the greater was its tendency to supercool. In particular, it was found that 1:3:5 tri-α-naphthyl benzene (subsequently referred to as TαNB in the text) spontaneously formed a glass on cooling its melt. The glass temperature of this material was found to be about 70°C. It was further observed that this irregularly shaped hydrocarbon was very slow to nucleate in a dilatometer whatever the supercooling.

The present work on this interesting Van der Waals glass-former has yielded some novel results. The facility with which crystallization can be by-passed in this material permits the two kinds of solidification phenomena to be studied. The continuous type of transformation is reported in a companion paper[4] on the viscous and viscoelastic behaviour of this compound. The present investigation is mainly concerned with the kinetics of the discontinuous phase change, from the metastable liquid to the crystalline state. However criterion for the glass formation[5,6,7] in this pure hydrocarbon will be discussed in relation to a variety of other glass forming materials. At the same time, the results of viscosity[4] and crystal growth rate measurements will be used to examine current theories

of melt solidification.[8,9,10] Particular emphasis is placed on the rate phenomena which occurs in the temperature range where the crystal growth is believed to be transport dominated.

In the past, measurements on a single substance have seldom covered a wide enough temperature range, from small to large supercoolings, in order for an extensive analysis to be conducted. At the same time, pertinent physical properties have been frequently lacking in many studies. The purity of the materials used has often been moot. Work has frequently been carried out at different times by a variety of investigators. By conducting all our experiments on the same batch of material we hope to have eliminated some of these variables.

A preliminary communication on this topic has just been published.[11]

Experimental

Materials--The compound 1:3:5 tri-α-naphthylbenzene was prepared and purified as described in the literature.[2,4] The melting point of crystals of this material conducted on a Kofler microscope hot stage at very slow heating rates, was found to be 199°C. An identical value was independently obtained from calorimetric studies[12] on this same material. The boiling point, T_b, of this substance is about 590°C (estimated by extrapolation of the vapor pressure data[2]).

Crystal morphology--X-ray studies[13] reveal that TαNB crystals formed at all degrees of supercooling are monoclinic with the space group P21/c. There are four molecules in the unit cell. These crystals

have a similar structure to those previously reported from toluene solutions.[2] Growth occurs in the c axis direction, corresponding to the shortest lattice parameter in the unit cell. The interplanar (011) spacing in this direction is 8.4 Å. The crystals are biaxial with a comparatively small optic axial angle. The refractive index in the growth direction is less than that transverse to it. Single crystals consist of thin platelets but thicker lath-shaped specimens are also encountered. Crystal growth proceeds without noticeable thickening. An ideal or perfect crystal is illustrated schematically in Figure 1. The width of the crystals, to a first approximation, depends on the crystallization temperature and range in width from a few microns to several hundred microns. Crystals possess extinction angles of approximately 4° with respect to their long (c) direction. Twinned crystals are sometimes obtained when the crystallization is conducted about 190°C and above. No polymorphic forms were found in TCNB although more than one kind of crystal was anticipated.[2] The crystals did not undergo any optically observable solid-solid transformation between room temperature and the fusion point when examined with the polarizing microscope. Limited X-ray diffraction measurements[13] revealed that no second crystalline phase was present in the temperature region of interest to us. Furthermore, when TCNB was examined in $CHCl_3$ solution by thin layer chromatography on silica gel, no phase separation was observed.

Crystal surfaces were examined by optical microscopy for screw dislocation growth at magnifications up to ×500 but the results were negative. Crystals tilted on a Leitz Universal stage at lower magnifications (×200 and below) did not reveal this type of imperfection. A

more detailed morphological study of the nature of the crystal interface must await electron microscopical investigations.

The crystalline texture of TONB changes with the extent of the supercooling. Over the crystallization interval (197° to 95°C) a gradual transition in morphology is observed as the growth temperature is lowered either slowly or in a stepwise manner. Single crystals (Figure 2a and 2b), crystalline aggregates (Figure 2c) and spherulites (Figure 2d) are found. The crystalline habit illustrated in Figure 2b is found less frequently than that in Figure 2a. The crystalline structure of both types of crystals are indistinguishable. The spherulites consist of radial arrays of crystals. Since the spherulitic birefringence has a negative sign, the orientation of the crystals comprising the spherulite is the same as in the mono-crystals. X-ray evidence also indicates that the c crystallographic axis lies radially in these spherulites.

A single crystal changes into a spherulitic array when this crystal is quenched to, and held at lower growth temperatures where the spherulitic structure is the stable form or habit. Fibrillation of the smooth crystal interface occurs as the crystal transformation proceeds under these new conditions. The observed change in morphology is shown for a crystal initially formed at 193°C (Figure 3a) and then cooled to, and held at 140°C while growth proceeds, as in Figures 3(b) to 3(d). Close inspection of the new crystal habit in Figure 3d reveals faceted profiles resembling those observed for the single crystal. These crystal

profiles become more obvious when the temperature is raised to 190°C when further growth occurs showing well defined crystallographic faces in the emanating array of crystals illustrated in Figure 3(e). Figure 3(f) shows the growth form which has occurred at 115°C on a single crystal initiated at an elevated temperature. The crystal facets at the melt-liquid interface in this example are again worth noting. Proturbances normally occur at the (011) faces causing multiple nucleation and the development of a radial arrays of crystals at the growing interface. The crystals do not normally increase in width as much as this series of photographs suggests. These examples clearly demonstrate that the spherulite is the preferred crystal habit at large supercoolings where the viscosity of the melt reaches a several hundred poises. The work presented in the following section describes the crystal growth kinetics and indicates how they vary with the crystallization conditions.

Crystal growth rate measurements--The TONB crystals were fused at 220° for 3 to 5 minutes and then crystallized isothermally on a thermostatted Köfler hot stage mounted on a Reichert polarizing microscope. Stability tests[2,14] indicated that these fusion conditions did not adversely affect this material. Since the melt did not spontaneously crystallize on cooling, nucleation was induced artificially by either seeding or quenching below T_g followed by upquenching to the crystallization temperature. Once the melt was nucleated, the rate of growth of a suitably oriented crystal was measured as a function of time at magnifications of ×100

or ×250, respectively. The growth rate of single crystals was measured in the c direction (see Figure 1). Nucleation occurs on the (011) crystallographic faces. In the case of the spherulites, the rate of advance of the overall interfacial profile was measured. Frequently measurements were made on a given crystal or spherulite which was partially melted back and recrystallized. Throughout our measurements we endeavoured to determine the rate of growth of those crystals which appeared in isolated regions of the melt so as to minimize potential stresses which could be transmitted by vicinal crystals. The crystallization kinetics of small molecules such as TCNB are more sensitive to such stresses than are polymeric materials.[15] Crystal growth rate measurements were also made with and without a cover glass on the crystallizing TCNB and similar growth rates were obtained on isolated crystals in both experiments. The crystal front advanced linearly with time under both these conditions.

Variations in crystal growth rate were found at any given temperature. The fluctuations in rate were largest at the higher crystallization temperatures. An unsuccessful attempt was made to obtain a simple correlation between crystal width and solidification velocity. It was further observed that the rate of growth of a particular crystal could be accelerated by disturbing it. Above 190°C approximately, twinned crystals were observed in addition to single crystals. The solidification rates for both twinned and disturbed crystals are omitted from Figure 4 which contains the averaged growth rates for single crystals.

aggregates and spherulites grown under the most favorable conditions. Some typical rate values are also given in Table I.

The rate, which is expressed in cms/hr., passes through a maximum value, T_{max}, around 175°C. The increase in the crystal half-length is recorded in order to be consistent with the radial increase in spherulites. The reproducibility of crystal solidification velocities to the right of T_{max} is better than ± 50%. The scatter was greatest at the smaller supercooling. To the left of T_{max}, the variation is about ± 10%. No rate measurements were made below 95°C because solidification was very slow from this point down to the glass temperature (T_g = 69°C). Estimates of this rate of crystallization are mentioned in the discussion.

Within 2°C or less of the melting point (T_m = 199°C), no perceptible crystal growth was observed over a period of days while the contour of the crystal faces remained unchanged. Lowering the temperature on these crystals prompted growth. With few exceptions, the crystal shapes or profiles remained unaltered for any growth temperature, until impingement occurred with other crystals. Sometimes as crystals approached each other their growth was accelerated presumably because of "built-in" stresses. This behaviour was most pronounced in densely nucleated areas of the sample or when a considerable amount of the melt had been transformed.

Although a spherulitic habit is the preferred one when the viscosity exceeds a few hundred poises, it is still possible to grow single crystals at high supercoolings for a limited time under very viscous conditions before they transform to spherulites. In these circumstances, the measured rate of crystal growth lies within experimental error of the normal spherulitic growth rates. As crystallization proceeds, proturberances in the shape of the interface gradually result in the single crystal interface changing to a spherulitic habit. The onset of instability at the (011) crystal faces

generally occurs more readily the larger the thermodynamic driving force. The crystals comprising a spherulite are distinguishable as they emanate from a central nucleus. Microscopical inspection of these crystal between crossed polars indicates that the crystals are closely knit.

TONB doped with small traces of o-terphenyl (which acted as a non-crystallizable impurity in these circumstances) only showed a significant decrease in growth rate notably at the lower crystallization temperatures where the habit is spherulitic. When larger quantities of o-terphenyl were added, the deceleration of the growth rate was marked.

Solubility measurements--Solubilities of TONB in benzene were determined at several mole fractions. The mixtures were made by weight in pyrex tubes and sealed under vacuum after the tube and contents were embedded in solid carbon dioxide-acetone mixture. Samples were reweighed after sealing to check if solvent loss had occurred. Precautions were taken to exclude moisture prior to sealing the tubes. The average solution temperatures are recorded in Table II. These values correspond to temperatures where the last traces of solid disappeared when the thermostat temperature was slowly raised in a step-wise manner (in about 0.1°C intervals) while the samples were rocked mechanically. From the results in Table II, the solubility of TONB can be represented within experimental error by a van't Hoff equation in the integrated form:

$$\log (x_1) = - \frac{1716}{T} + 3.636 \qquad (1)$$

where x_1 is the mole-fraction of TONB in benzene. The straight line passes through the melting temperature at $x_1 = 1$ (which is also listed in Table II). The heat of solution, ΔH_s, of TONB is calculated from the slope of the line to be just over 9.1 k.cal./mole, whereas the heat of fusion, ΔH_f, determined by differential scanning calorimetry[12] was found to 10.0 k.cal./mole (measured on the same material).

Discussion

Crystallization Kinetics

Preliminary. The solidification velocity, G, of a crystal in contact with its melt has been represented by the classical equation[16,17,18,19]

$$G = G_0 \exp\left(\frac{-\Delta F^*}{RT}\right) \exp\left(\frac{-\Delta G^*}{RT}\right) \qquad (2)$$

where G_0 is a parameter usually considered constant and ΔF^* represents the activation energy characteristic of transport of material across the liquid-crystal interface. For practical analysis, ΔF^* is usually identified with the activation energy for viscous flow or self-diffusion in the liquid. ΔG^* is the motivating free energy for nucleation. The term $\Delta G^*/RT$ can be written in a variety of forms depending on the crystal geometry and the mechanism of crystal growth. For example, the driving force is linear in ΔT^{-1} for two-dimensional surface nucleation or it varies as ΔT^{-2} for a three-dimensional mechanism. The supercooling below the thermodynamic melting point (T_m) is ΔT.

Detailed consideration has been given to other crystal growth mechanisms in a recent review article[8] which also presents a diffuse interface theory to describe all existing experimental data on the solidification of metals, organic and inorganic materials. We shall examine our results in the light of this theory, which in essence predicts a transition from a stepwise growth mechanism at low supercoolings, to a "continuous" mechanism at higher supercoolings. For continuous growth, G, is expressed

by an equation of the form:

$$G = \frac{\beta D \Delta H_f \Delta T}{b_0 R T^2} \tag{3}$$

where β is a molecular accommodation coefficient, D is the liquid diffusion coefficient, b_0 denotes the interplanar crystal spacing in the growth direction and ΔH_f is the heat of fusion. Although this equation strictly applies to small supercoolings, these authors have applied it at large supercoolings. They believe that the magnitude of the driving force determines the type of interface, there being an infinite or continuous range of possibilities between smooth and rough surfaces. The criteria for the surface morphology varies with the material and the driving force for a given superccoling.

The kinetics of solidification by a screw dislocation mechanism[8] has been expressed as

$$G = \frac{\beta(1 + 2g^{1/2})}{g} \frac{D \Delta H_f^2 (\Delta T)^2}{4\pi T^2 R T \sigma V_m} \tag{4}$$

in which g, the interface diffusiveness, is less than unity,[‡] V_m is the molar volume of the solid, and σ is the crystal surface energy. Other equations describing the freezing velocity of a crystal in terms of atomic mechanisms have been discussed periodically in the literature[10,20,21].

The Jackson theory[10], pertaining to interface roughness, is particularly of interest since the predictions arising from it are consistent with observed morphological features. These predictions

---

[‡]For a sharp interface, g is of order 1.

can be made on the basis of a knowledge of the entropy of fusion, the crystal structure and the bonding in the material in question.

Among the most recent and significant developments of nucleation theory are the statistical mechanical formulations by Pound and co-workers[22,23] which are concerned with homogeneous nucleation from the vapor phase. In this theory they considered quantum mechanical contributions to the free-energy of formation of nuclei, arising from their absolute entropy. A similar treatment of liquid-solid transformations would be most informative but the problem may become intractable for "complex" molecules.

Analysis of Results

Crystallization Kinetics. Since the crystals of TCNB exhibit a lamellar habit,[17] the form of $\exp(-\Delta G^*/RT)$ becomes $\exp(-BT^*/T\Delta T)$ if nucleation occurs by a coherent surface nucleation mechanism, where $B = 4b_0\sigma^2/\Delta H_f k$. The symbols have already been defined. For a three-dimensional growth mechanism, the form is $\exp(-B'T_m^2/T(\Delta T)^2)$ with $B' = 32\sigma^3/\Delta H_f^2 \cdot k$.

The crystal growth rate to the left of the maximum (Figure 4) is normally believed to occur at the rate allowed by the diffusive processes in the melt. The rate of this transport process is commonly assumed to have the Arrhenius form $\exp(\Delta F_\eta^*/RT)$. For TCNB, the logarithm of the experimentally measured viscosity values[4] are plotted against 1/T in Figure 5. These results clearly indicate that there is a very pronounced change in the apparent activation energies of flow as the temperature decreases. Calculated values are listed in Table III. The nonlinear

form of these data and the magnitude of ΔF_η^* suggest that co-operative processes must be involved in the liquid. These results clearly indicate that the temperature dependence for transport measured over a wide temperature range, up to and <u>including</u> the T_g region, cannot be approximated by the Arrhenius equation. At high temperatures (above T_m) the melt viscosity is relatively insensitive of temperature and the flow process can be accounted for with a realistic value for ΔF_η^* of about 7 kcal/mole or perhaps even less at still higher temperatures. The viscosity of metals[24] can nearly always be represented by a log η vs 1/T plot in the experimentally accessible temperature region. In contrast to metals, however, irregularly shaped organic molecules[1,2,3] show a rapid increase in viscosity on traversing the metastable liquid region. The "anomalous" behavior has been ascribed to the presence of non-crystallizable transient clusters[2,3] in the metastable liquid which progressively increase in number and perhaps size as the supercooling increases. Their lifetime is of sufficient duration to affect viscous flow.

The empirical Vogel[25] or Doolittle[26] free volume type relationship, which invokes an additional parameter (compared with the Arrhenius equation), cannot adequately account for the measured change in viscosity of TαNB over the fifteen logarithmetic decades. This point has been dealt with in some detail in the first paper[4] in this series which stringently tests free volume concepts. Indeed, a review paper[27] of flow properties of a variety of materials points to the inadequacy of a plot of log η vs 1/T or even $1/(T - T_\infty)$ to represent any data which cover <u>a very wide range</u> of fluidities. Here T_∞ is some hypothetical reference temperature above 0°K. Unfortunately the best literature data[28,29,30] are not as extensive as the TαNB measurements which provide a real test of liquid transport properties. The magnitude of the viscosity range covered is probably <u>more</u> important than the extent of temperature range because at high temperatures the flow behaviour is not very temperature sensitive.

Over much of the temperature interval corresponding to the transport dominated crystal growth region, the viscosity can be described by a free volume expression. If it is assumed that crystal growth is viscosity dominated then the first exponential in equation (2) becomes $\exp[-C/(T - T_\infty)]$ (with the appropriate pre-factor) so that the equation for crystal growth by a surface nucleation mechanism may be written as

$$G = G_0 \exp\left(\frac{-C}{T - T_\infty}\right) \exp\left(\frac{-BTm}{T\Delta T}\right) \qquad (5)$$

For three dimensional growth it becomes:

$$G = G_0' \exp\left(\frac{-C}{T - T_\infty}\right) \exp\left(\frac{-B'Tm^2}{T\Delta T^2}\right) \qquad (6)$$

The parameter C in these equations may be written as Q/R if the modified transport exponential is to be considered as a "modified" Arrhenius relationship. Clearly a simple Arrhenius term as in equation (2) will not suffice unless a continuously variable activation energy is used. In a sense, this energy may be reconciled with the free volume concept in which the loss of molecular mobility brought about by the decreased free space in the liquid as the temperature is lowered is paralleled by a concomitant increase in the interaction energy between molecules because of proximity effects. However, it is necessary to reiterate at this stage some important results from the first paper. From free volume notions of transport in liquids we have demonstrated that a redistribution of free volume can take place at constant temperature for $T \propto NB$. It therefore follows that at low temperatures within 70° or less of T_g (and indeed below the

one minute T_g) that the diffusive process in viscous systems can hardly be regarded as thermally activated in the commonly accepted sense. Cohen and Turnbull[6] have remarked on the nature of this process in their mathematical consideration of a hard sphere free volume model of the liquid state. In practice we find that the parameters C and T_∞ which describe the macroscopic viscosity, do not correspond to those found to fit the growth rate data. However, an expression which invokes this same form can be used to reproduce the crystal growth rates of TCNB (see equation (5)).

The following procedure was used in fitting the experimental data. By a Williams-Landel-Ferry analysis[29] of the crystal growth rates at large supercoolings between $T_g + 25°$ and T_{max}, a reduced plot of the form $(T - T_S)/\log (G/G_S)$ against $(T - T_S)$ is made to determine the slope and intercept of the straight line in order to obtain the approximate values for the constants C and T_∞. G_S is the growth rate at the chosen reference temperature, T_S. Then rearranging equation (5) and plotting $\log G + \frac{C}{2.303(T - T_\infty)}$ versus $1/T\Delta T$ gives an approximate value of B. With this B, the temperature dependence of the transport process involved in crystallization can be written as $G' \equiv G \exp (\frac{BTm}{T\Delta T})$. From these nucleation corrected G' values, a more accurate estimate of C and T_∞ are made as illustrated in Figure 6 for the equation (5). In turn, a better value for B is obtained from the slope of the plot in Figure 7. This process is repeated once more and the deduced constants for equations (5) can be used to fit the crystal growth rate data within experimental error perhaps with the exception of results within a few degrees or so of the threshold region, 197°C. This difficult region requires further and more detailed study. The derived growth rate

equation which reproduces the majority of the data has the form:

$$G = (8.55 \times 10^4) \exp^{-1570/(T - 300)} \exp^{-20,400/T(472 - T)} \qquad (7)$$

where G is expressed in cm/hr. The solid line in Figure 4 is calculated from this equation. The growth rate at T_g is estimated at 0.02 Å/day.

Figure 8 illustrates some of the key relationships arising out of the foregoing analysis. All plots are made over the same temperature interval for data to the left of T_{max}. The graphs clearly show that the temperature dependence for viscous flow and the nucleation-compensated transport-dominated crystal growth G' differ significantly. Curves A and B indicate the form of the relationships for the experimental data corrected for the two and three dimensional nucleation cases respectively. Curve C illustrates the shape of the uncorrected reduced plot of $\log(G/G_S)$. This plot does not assume any nucleation model. It is therefore apparent from Figure 8, that the measured temperature dependence of viscous flow does not quantitatively describe the crystal growth of TCNB in the temperature region between T_g and T_{max}. The rate determining step must be transport motivated, but not in the manner directly reflected by the measured viscosity.

The disparity between the temperature dependences of the macroscopic viscosity and transport dominated crystal growth may be further highlighted by an alternative analysis. This method assumes a specific growth mechanism and involves a wider range of temperature than that outlined in Figure 8. Direct substitution of the measured

viscosity values for the transport term in equation (5) gives

$$\log G\eta = \log G_0 - \frac{BTm}{T\Delta T} \qquad (8)$$

A plot of log $G\eta$ vs. $1/T\Delta T$ is illustrated in Figure 9. Much of the linear higher temperature portion of this graph corresponds to the nucleation controlled growth rate region plus the region through T_{max}, where the viscosity does not exhibit a strong temperature dependence. There is a marked departure from this linearity below 140°C approximately where the viscosity has a pronounced temperature dependence. One might argue that the measured growth rates are too high at these lower temperatures because of the gradual change in morphological habit to a stable spherulitic form in this interval. Since we have demonstrated experimentally that single crystals can grow at the same rate as spherulites, in the same temperature region, this cannot be the reason. Impurities cannot be responsible for the deviations below 140° because impurities suppress the growth rate. This would mean that a purer sample than our TCNB would crystallize even faster thus causing a more marked deviation than presented in Figure 9. Clearly, it cannot be argued that the crystal growth rate allowed by diffusive processes is quantitatively reflected in the melt viscosity over the entire crystallization interval.

Another approach[24] related to equation (8) may be invoked in which a variable crystal surface site factor, f, is introduced to account for the non-linearity of the log ($G\eta/T$) vs. 1/T plot (not shown). Although a change in f is expected and observed with increased undercooling, this approach presupposes that it is correct to directly represent the diffusive

process in crystallization by $1/\eta$. It is important to reiterate at this stage that G is not directly correlated with $1/\eta$ and that invalid generalizations have resulted in the past because experimental data has been too limited[30] to adequately test this relationship.

In view of recent considerations[8] of the molecular mechanism of solidification it is pertinent to examine our results further using the concepts embodied in equations (3) and (4). We shall in the interest of space only present our data for equation (3). The results are plotted in Figure 10 in the form $G\eta/\Delta T$ against ΔT. The overall shape of this graph indicates that the results are best described by an exponential relationship. The threshold in the solidification rate, within two degrees or so of T_m, is in agreement with a surface nucleation theory which predicts a barrier to nucleation. Although there are uncertainties about the absolute values for G in the region of small supercooling, the observed trend in Figure 10 is sufficiently different from the "universal" pattern in Figure 1 of reference 8 to invalidate it for TQNB. Admittedly there is an apparent kink in the curve of Figure 10 around $\Delta T = 15^\circ$ but its magnitude (compared with experimental error in the measurements) does not permit us to attach any real significance to it at present. The arbitrary line in the magnified insert should rise less steeply than we have indicated. Further growth rate studies and a more detailed inspection of the crystal topography should be made, but the present analysis of our results indicates that they are best described by an exponential relationship and not by the proposed mechanism of Cahn, Hillig and Sears[8].

A kinetic limit to growth at small supercooling has also been reported for salol[29,32,33] but it is also pertinent to point out that other crystallization studies on this material[8] have been interpreted on the Cahn model. At present, controversy exists over salol.

Molecular Parameters from the Rate Equations

Over the temperature range where the free volume expression fits the crystal growth results, the calculated parameters for crystal growth are $v_o = 0.848$ cm^3/g, $b = 0.84$ and $T_\infty = 300$°K. The viscous flow parameters are $v_o = 0.810$ cm^3/g, $b = 4.18$ and $T_\infty = 200$°K. The Doolittle parameter b, according to Cohen and Turnbull,[6] is a measure of the minimum hole size necessary for mass transport in the liquid. The parameter v_o represents the occupied volume. Rationalizing our result, we note that because b for viscous flow is the larger, more cooperative motions are required for flow than for crystal growth. At high temperature (Figure 8), where there is more free available volume, mass transport in viscous flow changes more rapidly than it does in crystal growth. It appears reasonable that v_o should be the larger for crystal growth, because in the vicinity of a growing crystal face the local probability for density rarefactions can be lowered by virtue of the space-consuming nature of this substrate. The crystallization of a molecule like TCNB must involve more than simple translational motion across this interface. Because of its shape, it may rotate about an axis (z) perpendicular to

the central benzene ring if the naphthalene groups are inclined at less than the assumed 45° angle to this ring[2]. Even if a molecule can rotate independently of its neighbors, because of volume requirements two or more molecules may move in concert[35]. In this way half the rotational entropy survives because the effective combined rotator, for instance in the two molecule case, has about twice the moment of inertia. If one considers the TCNB molecule as disc-shaped with non-equivalent faces, then it is clear that rotation about an axis transverse to the z axis will be necessary to bring the molecule into a suitable orientation for incorporation into the crystal lattice. Staveley[34] has made a related proposal. We suggest that the activation energy for rotary diffusion may be the rate determining step in the addition of molecules to the substrate.

The crystal edge surface energy σ was calculated from equation (7) as 14.1 erg/cm^2 with a slightly lower value of 11.7 erg/cm^2 at smaller undercoolings. The surface energy calculated from the slope of the nucleation controlled high temperature end of the straight line in Figure 9 is 13.7 ergs/cm^2 in good agreement with the former value. This value is higher than that deduced from the crystal growth rate studies by Sears[36,37] and Hillig[38] for other small molecules but this may be partly due to the different crystal geometry which they assumed. The value of σ_h for homogeneous nucleation[33] can be estimated from the semi-empirical relationship:

$$\sigma_h = \gamma \Delta H_f / N^{1/3} V_m^{2/3} \qquad (11)$$

connecting solid-liquid interfacial energy and bulk properties. The value of γ lies between 1/3 and 1/2, but it is probably closer to 0.4,

in which case $\sigma_h \sim 37.9$ ergs/cm^2. Equation (11) is solved with $V_m = 377.8$ cm^3 and $\Delta H_f = 10^4$ cal/mole. If it is assumed that $\gamma = 0.3$ as Sears[36,37] has done in his experiments with durene and p-toluidine, then the lower limit for σ_h is 28.4 erg/cm^2 approximately.‡ This value is just over 2σ. In most studies relating to single crystal solidification kinetics, σ has been found to be much less than σ_h.

Remarks on the Crystal Morphology and Growth Mechanism. Figure 2 demonstrates that TCNB crystals have well-defined crystallographic surfaces of the type illustrated in Figure 1. These figures suggest that the crystal growth is not limited by heat flow conditions and so provides useful information on the nature of the solidification process per se. The radiating crystals within the spherulites in Figure 3 have profiles closely allied to those of the lath-like single crystals just shown. These simple observations of the morphological features of solidified TCNB suggest that a continuous growth rate process is unlikely.

It is informative to inquire further into the nature of these faceted interfaces. During the solidification process the molecules lose rotational, positional and configurational entropy so that their arrangement at the liquid-solid interface may be just as important as the

---

‡It would be interesting to compare our estimated σ_h with that determined from droplet experiment, but it is thought that TCNB would not lend itself readily to homogeneous nucleation studies because nucleation directly from the melt is not spontaneous even at large supercoolings. Either the barrier to nucleation is too high, or the temperature region of homogeneous nucleation lies too close to, or even below T_g, in which case comminutive methods may not be fruitful.

number of molecules present. This in turn implies that molecular crystals have high entropies of melting and according to current theories[10] of interface morphology high entropies of fusion can be associated with an atomically flat crystal face. Jackson[10] has presented a statistical mechanical model in which the interface roughness is described in terms of a parameter, α, which is given by

$$\alpha = \xi \Delta H_f / RT_m \qquad (12)$$

where ξ is a geometric coefficient which usually lies between 1/2 and 1. With $\xi = 1$ we find that $\alpha \sim 10.7$ ($\equiv \Delta S_f/R$) which is in keeping with the prediction and observation that large flat crystal faces are associated with materials for which $\alpha > 2$. This result may be interpreted from the standpoint of theory, that there are few extra atoms or holes in the crystal surface and that minimum or almost minimum free energy conditions prevail. For all metals $\alpha < 2$ and this implies that they should have rough surfaces in contact with their liquids. It has been shown recently that if molecular crystals have low α values[39] then they too freeze with rounded interfaces as this theory[10] predicts.

The crystal interface diffuseness may also be analyzed as suggested by Cahn.[8] Since the kinetics conform to a two dimensional mechanism, the supercooling corresponding to perceptible growth, ΔT_{go}, for which the energy barrier to nucleation is assumed to be 50 kT,

enables us to estimate a surface roughness of $g \sim .08$ with the surface energy of 14.1 erg/cm^2 and $V_m = 376.6$ cm^3 in the equation:

$$g = \frac{50k\,\Delta H_f\,(\Delta T)_{go}}{\pi\sigma^2 b_o V_m} \qquad (13)$$

in which the terms have already been defined. An identical value is calculated at T_{max} of Figure 4 where the supercooling is about 25° and $V_m = 375$ cm^3 for an assumed barrier to nucleation around 40 kT. It may be concluded that this invariance of g implies that the interface is not changing in character as ΔT is changed.

Any calculation of the barrier to crystal growth must contain the contributions from both exponentials in the growth rate equation. At 2° and 25° supercooling, we calculate from equation (7) that the ΔG^* term contributes 22kT and 3kT respectively. An estimate of the influence of the transport term (made from Figure 5) at ΔT = 2° and 25° is about 24 kT and 35 kT respectively. The total barrier to growth is a composite of both these terms and is therefore about 46 kT and 38 kT respectively for 2° and 25° supercooling. At T_g the ΔG^* contribution is negligible in comparison with the values for ΔF_η^* of 135 kT approximately. These values agree favorably with the assumed values used in equation (13). Although a high kinetic barrier is a stated requirement for surface nucleation, it is questionable if the barrier to the formation of a step on a crystal substrate surface can be properly identified with that witnessed in the formation of a new phase. We have already pointed out that TONB does not nucleate spontaneously on slowly cooling the molten phase even to the glass temperature. However, it is a fact that once the melt is artificially nucleated, growth does occur.

From the ratio of the edge surface energy σ to the estimated homogeneous surface energy σ_h another estimate of g can be obtained

from the relationship $g^{1/2} = (\sigma/\sigma_h)$. For $\sigma = 14.07$ and $\sigma_h = 37.9$ erg/cm^2 then $g = 0.14$. If a lower value of $\gamma = 0.3$ is assumed then $\sigma_h = 28.4$ and $g = 0.25$. From the Cahn theory the number of atomic layers, n, in the interface transition region in the crystal is now calculated to be less than unity from the relationship:

$$g \sim \frac{1}{8} \pi^4 n^3 \exp\left(-\frac{1}{2} \pi^2 n\right) \qquad (14)$$

Although the values of g and n compare very favorably with the best literature values[8] they do suggest a less than smooth interface since g falls short of unity. In this respect, the theories of Jackson and Cahn are not immediately reconcilable.[‡] However, the existence of a rough surface does not avoid the necessity of growth by layer spreading though a perfect crystal surface must grow by a two dimensional mechanism.

Optical microscopy studies of crystal surfaces do not favor the screw dislocation mechanism as a significant factor in crystal growth in the c direction but it is hoped that a more detailed knowledge of the lath-like nature of the crystal interface will come from an inspection of these surfaces with high resolution electron microscopy. The layered nature of the broad crystallographic faces is consistent with the proposed surface nucleation mechanism with its attendent threshold kinetics for $\Delta T < 2°$. We do not wish to imply dogmatically that screw dislocation growth is not possible in TCNB but we do state that if growth is observed at small supercoolings $< 2°$, then the crystals so formed will fall short of perfection.

[‡]Jackson, Hunt and Uhlmann have very recently communicated to us that they find the assumptions involved in the theory of Cahn and co-workers[8] limit its applicability to second-order phase transformations. Jackson, et al have repeated Cahn's analysis applying the formalism of his approach to first order phase transformations. A computer plot of g vs. n for both versions of the theory almost superimpose except for small $n < 2$, where the revised theory gives unacceptably high values for g, which are not consistent with experimental findings or with the surface roughness model[10,19].

The fact that deliberate additions of traces of impurity such as o-terphenyl brought about no appreciable reduction in the crystal growth rate (within experimental error) in the 180-190°C range suggests that these heterogeneities are not strongly adsorbed on the crystal surface and can readily diffuse away from the growing (011) faces. At the larger supercoolings where the viscosity of the medium is higher and the crystal habit spherulitic, the impurities are less mobile. The impurity phase builds up at the interface slowing down the freezing rate of the TCNB since the probability of impurity uptake is greater at these lower temperatures.

Comparisons of the macroscopic crystal dimensions (width) at the same growth rates but at different diffusitives to the right and left of T_{max} (Figure 4), indicate that the crystalline texture cannot be quantitatively explained in terms of existing concepts of impurity segregation[40] at an interface. The ratio of crystal widths at corresponding growth rates on either limb of Figure 4 decreases as the growth rate increases, but differ in magnitude from the measured melt viscosity ratios, under corresponding conditions, by almost 10^3. All crystal widths were measured on spherulites of the type illustrated in Figures 2 and 3 in order to validate the comparison in similar morphologies.

The observations on the incidence of spherulites in viscous TCNB raises questions about their origin. In a "pure" hydrocarbon impurity segregation can hardly be a main contributor. The effect of a changing motivating or driving force in nucleation, coupled with a changing site factor, f, with increasing supercooling must also play an important

role in determining the different crystal habits and crystal dimensions. Furthermore, the highly specific breakdown of the crystal interface (Figure 3) suggests that theories relating to interfacial profiles should not neglect the anisotropy of the system. The slow growth rates in TONB suggest that heat flow is unlikely to be a dominating factor in producing the observed morphology.

Remarks on Glass Formation in TONB. Although the glassy nature of this material has been discussed in some detail in the first paper,[4] there are further pertinent parameters peculiar to vitreous TONB and other related materials which are presented here. These characteristics of glass forming materials have been the subject of many papers. However, it is important to note that many of these parameters cited in literature refer to polar organic, or inorganic substances so that it is not surprising to find that some of these empirical constants are different for a Van der Waals liquid.

In particular, the viscosity of TONB at T_g ($10^{11.6}$ poises) is lower than that usually cited for glassy materials (10^{13} poises) in this region. Furthermore, the ratio $T_b/T_m = 1.83$ is less than 2.0 which is a lower limit quoted for other glass formers.[6] This lower ratio and lower viscosity at T_g can be rationalized on the basis that the bonding energy in a non-polar molecule is probably less than that in a polar one. The glass temperature for TONB is about 0.73 T_m, which is similar to that found for o-terphenyl (0.75 T_m) by Greet[41]. Because of the facility with which TONB passes into the vitreous state on cooling, without the onset of sensible homogeneous nucleation, it must be concluded that either a high kinetic barrier to nucleation exists or that the position of the rate of nucleation-temperature curve lies near, or below, the glass temperature. For this material T_{max}/T_m (~ 0.95) is higher than the norm (~ 0.8). Other parameters such as $T_g/T_b \sim 0.4$ and $\Delta H_{vap}/kT_m = 29.7$

agree favorably with the values cited by Greet[41] for o-terphenyl, but differ from those quoted for other glass forming materials.[42‡] However, the reduced glass temperature, $\tau_g = kT_g/\Delta H_{vap} = 0.0243$ for TQNB, is lower than that found for o-terphenyl[41] ($\tau_g \sim 0.0333$) and is characteristic of this parameter for other glasses.* While it may be stated that the parameters cited for TQNB do not seriously contravene the generalizations relating to vitreous behaviour, it is worthwhile examining this material in the light of recently developed reduced fluidity concepts of the liquid state.[42]

A fluidity function, β/η, derived from a free volume model by Turnbull[41]

$$\beta/\eta \sim 1/\eta \ (kT/\Delta H_{vap}) \ \sim (\beta)/\eta$$

where

$$\beta = (mT)^{1/2} \ v^{2/3}$$

is used to examine our data. In the above equations, m is the molecular weight, τ the reduced temperature, v the specific volume, v_o the occupied volume, and v_f the free volume. The molecular transport properties of Van der Waals liquids of varying degrees of complexity are compared with some "simple" molecular substances in Figure 11. Literature data[42] on this subject are sparse. Our analysis of some viscosity data[43] for cis-decalin (with a $\Delta H_{vap} = 9.84$ kcal/mole derived from Rossini's[44] vapour pressure measurements) falls in line with "simple" molecular

---

‡ $0.25 < T_g/T_b < 0.33$.

* $0.0189 < kT_g/\Delta H_{vap} < 0.0263$

liquids. We find that asymmetric Van der Waals liquids are displaced in a fashion which probably depends on their anisotropy and molecular complexity. Although 1:3:5 tri-phenylbenzene[45] readily crystallizes, its fluidity behaviour practically coincides with that of TOMB, while o-terphenyl lies in an intermediate position with an anomalously high τ_g. Noteworthy is the much steeper dip in the fluidity function, log (β/η), in the case of TOMB, although o-terphenyl which is also a glass former, seems to have similar characteristics. This fairly abrupt decrease occurs in the lower temperature region where the relaxation processes are becoming more severely hampered due to the diminution in the free volume for molecular movement[46] as T_g is approached. Generalizations on the glass forming ability of materials are pertinent here. For irregularly shaped molecules a large amount of disorder can be readily produced at the cost of little energy. This is further borne out in our preliminary studies of other non-polar organic compounds in which steric factors constrain elemental groups or portions of a molecule into non-planar configuration(s). Where substituents can adopt a planar configuration as in 1:3:5 tri-β-naphthylbenzene, TβNB, then crystallization[47] readily occurs on cooling the hydrocarbon melt to room temperature, in contrast to the glass forming habit of TOMB. The crystalline state is preferred when the molecular substitutents can take up lattice positions which are otherwise precluded by proximity effects in irregular shaped molecules. The melting point of TβNB is enhanced about 50° over that for the non-planar TOMB molecule of similar molecular weight.

Heat of Solution. Since the heat of solution, ΔH_s, calculated from equation (1), appears to be less than the heat of fusion ΔH_f, ideal solubility behavior is not found. It is surprisingly that a linear relationship exists between log x_1 and 1/T even though the ratio of molecular volumes of solvent to solute is about 1 to 5. Regular solution theory demands that this ratio should be between 1 and 2 if solute and solvent molecules are to be interchangeable on a quasi-lattice.[48,49]

Conclusions

1. The temperature dependence of mass transport in viscous flow is not identical with that for crystal growth over a wide temperature range.
2. Crystal growth in 1:3:5 tri-α-naphthylbenzene seems to proceed via a two dimensional surface nucleation mechanism.
3. The crystal edge surface free energy is found to be about 14.1 erg/cm^2.
4. An analysis of the atomic kinetics indicates that the surface roughness is probably less than one atomic plane at the crystal interface.
5. Free volume parameters calculated for crystal growth and viscous flow suggest that more co-operative motions are necessary for flow than for crystal growth.
6. The crystal morphology passes from a single crystal to a spherulitic habit with increasing supercooling. The spherulite (comprised of radial crystals) is the stable form at large supercoolings.
7. The maximum growth rate occurs around 175°C (24° below T_m). Growth occurs at an estimated value of 0.02 Å/day at the glass temperature (69°).
8. TCNB does not nucleate spontaneously on cooling its melt.
9. The glass-forming properties of TCNB provide a unique example of the behaviour of a sterically hindered Van der Waals liquid which displays reduced fluidity properties that differ from "simple" molecules.

Acknowledgements

J. H. Magill acknowledges support from ONR under contract no. Nonr 2693(00) and D. J. Plazek thanks NASA under Grant NsG 147-61 during these investigations. The authors are indebted to Drs. T. G Fox and H. Markovitz for helpful criticisms of the manuscript.

References

1. J. N. Andrews and A. R. Ubbelohde, Proc. Roy. Soc. A228, 435 (1955).
2. J. H. Magill and A. R. Ubbelohde, Trans. Faraday Soc. 54, 1811 (1958).
3. E. McLaughlin and A. R. Ubbelohde, Trans. Faraday Soc. 54, 1804 (1958).
4. D. J. Plazek and J. H. Magill, J. Chem. Phys. (to be published).
5. D. Turnbull and M. H. Cohen, J. Chem. Phys. 29, 1049 (1958).
6. M. H. Cohen and D. Turnbull, J. Chem. Phys. 31, 1164 (1959).
7. W. A. Weyl, Symposium on Nucleation and Crystallization in Glasses and Melts, edited by M. K. Reser, G. Smith and H. Insley, The American Ceramic Society, 37 (1962).
8. J. W. Cahn, W. B. Hillig and G. W. Sears, Acta Met. 12, 1421 (1964).
9. B. Chalmers, Principles of Solidification, John Wiley and Sons Inc., New York (1964).
10. K. A. Jackson, Liquid Metals Solidification, p. 174, ASM, Cleveland (1958).
11. J. H. Magill and D. J. Plazek, Nature 207, 70 (1966).
12. R. A. Marsella, private communication.
13. S. S. Pollack, private communication.
14. A. Leonard, E. McLaughlin and A. R. Ubbelohde, Chim. Ind. 89, 58 (1963).
15. J. H. Magill, J. Applied Phys. 35, 3249 (1964).
16. R. Becker and W. Doring, Ann. Physik. 24, 719 (1935).
17. J. D. Hoffmann, S. P. E. Transactions 4, 315 (1964).
18. D. Turnbull and J. C. Fisher, J. Chem. Phys. 17, 71 (1949).
19. M. Volmer and M. Marder, Z. Physik. Chem. 154, 97 (1931).
20. G. F. Bolling and W. A. Tiller, J. Applied Phys. 32, 2587 (1961).
21. W. K. Burton, N. Cabrera and F. C. Frank, Phil. Trans. Roy. Soc. A243, 299 (1951).
22. J. Lothe and G. M. Pound, J. Chem. Phys. 36, 2080 (1962).
23. S. J. Hruska and G. M. Pound, Progress in Solid State Chemistry 2, 117 (1965).

24. D. Turnbull, Transactions AIME 221, 422 (1961).

25. H. Vogel, Physik, Z. 22, 645 (1921).

26. A. K. Doolittle, J. Applied Phys. 23, 236 (1952).

27. G. C. Berry and T. G Fox, Fortschr. Hochpolym. Forschung., to be submitted.

28. M. Volmer and M. Marder, Zeit, fur physik. Chem. A154, 97 (1931).

29. O. Jantsch, Zeit fur Kristallographie 108, 185 (1956).

30. J. G. Morley, Glass Technology 6, 77 (1965).

31. M. L. Williams, R. F. Landel, and J. D. Ferry, J. Am. Chem. Soc. 77, 3701 (1955).

32. D. E. Ovsienko and G. A. Alfintsev, Kristallografiya 8, 796 (1963).

33. V. I. Danilov and V. I. Malkin, Zhur. Fiz. Khim 27, 1837 (1954).

34. D. G. Thomas and L. A. K. Staveley, J. Chem. Soc. 4569 (1952).

35. F. C. Frank, Sci. J. Royal College of Science, 25, 1 (1956).

36. W. K. Murphy, E. I. Hormats and G. W. Sears, J. Chem. Phys. 40, 1843 (1964).

37. G. W. Sears, J. Phys. Solids 2, 37 (1957).

38. W. B. Hillig, "Growth and Prefection of Crystals" edited by R. H. Doremus, B. W. Roberts and D. Turnbull, p. 350, John Wiley, New York (1958).

39. K. A. Jackson and J. D. Hunt, Acta. Met., 13, 1212 (1965).

40. H. D. Keith and F. J. Padden, J. Applied Physics 34, 2409 (1963).

41. R. J. Greet, "Liquid-glass Transition of Van der Waals System" Ph.D. Thesis, Harvard University, p. 163, 1966.

42. D. Turnbull and M. H. Cohen, J. Chem. Phys. 34, 120 (1961).

43. G. C. Berry (private communication).

44. D. L. Camin and F. D. Rossini, J. Phys. Chem., 59, 1173 (1955).

45. J. H. Magill (unpublished results).

46. T. G Fox and P. J. Flory, J. Applied Physics 21, 581 (1950).

47. J. H. Magill and D. J. Plazek (unpublished results).

48. E. McLaughlin and H. A. Zainal, J. Chem. Soc. 863 (1959).

49. E. A. Guggenheim, "Mixtures" Oxford University Press, p. 24 and 29, 1952.

Table I

Crystallization Velocity, G, as a Function of Temperature

T °C	G cm./hr.	T °C	G cm./hr.
95	9.74×10^{-6}	160	1.62×10^{-1}
100	4.03×10^{-5}	165	2.40×10^{-1}
105	1.12×10^{-4}	170	3.28×10^{-1}
107.5	1.68×10^{-4}	175	3.37×10^{-1}
108	1.92×10^{-4}	180	2.89×10^{-1}
110	3.33×10^{-4}	182.5	2.26×10^{-1}
115	6.86×10^{-4}	185	1.60×10^{-1}
120	2.08×10^{-3}	187	1.04×10^{-1}
125	4.20×10^{-3}	190	5.82×10^{-2}
130	8.88×10^{-3}	191	2.17×10^{-2}
135	1.70×10^{-2}	192.5	1.28×10^{-2}
140	2.96×10^{-2}	193	7.26×10^{-3}
144	4.20×10^{-2}	193.5	1.04×10^{-3}
150	8.40×10^{-2}	195	6.18×10^{-4}
155	1.40×10^{-1}	197	0

Table II

Solubilities of 1:3:5 Tri-α-Naphthylbenzene in Benzene

Dissolution Temperature °C	64.7	85.5	115.4	134.3	167	199
Mole Fraction TαNB	0.0211	0.0475	0.1262	0.2264	0.4579	1.0000

Table III

Apparent Activation Energies for Viscous Flow, ΔF_{η}^{*}, for TCNB

Temperature °C	300	200	95	69
ΔF_{η}^{*} kcal./mole	7.2	21	93	120

Legends to Figures

Figure 1 Isometric view of an "Ideal" TαNB crystal showing the (011) growth faces.

Figure 2 Morphology of TαNB crystals grown at (a) 192°C (X40), (b) 185°C (X50), (c) 180°C (X50), (d) 95°C (X40). Crossed polaroids.

Figure 3 Photomicrographs (a) to (d) illustrate the morphological transition from a single crystal habit (nucleated at 193°C) to a spherulitic array when the sample is quenched to, and crystallized isothermally at 140°C (X125). Photomicrograph (e) shows further growth of (d) upquenched to, and crystallized at 190°C (X40). Spherulitic growth at 115°C on both ends of a single crystal formed at an elevated temperature (X125). White light.

Figure 4 Crystal growth rate G, (cm./hr.) vs. crystallization temperature, T°C.

Figure 5 Arrhenius plot of Log (viscosity) in poises vs. 1/T°K for TαNB.

Figure 6 Reduced W.L.F. plot T-Ts/log(G'/G's) of the nucleation-corrected crystal growth rate data G' to the left of the growth-rate maximum at 175°C. G's is the growth rate at T_s = 100°C. T-Ts is the temperature difference from the reference point, T_s.

Figure 7 Growth rate data corrected for two dimensional surface nucleation, in the transport-dominated region between 170° and 95°C. T_∞ is the reference temperature (27°C) where crystal growth vanishes.

Figure 8 Temperature dependence of the reduced viscosity $\log(\eta/\eta_s)$ and transport-dominated crystal growth rate $\log(G/G_s)$ of TαNB. Curve A is corrected for two-dimensional surface nucleation, B is corrected for three-dimensional nucleation, and C is an uncorrected plot of the data. The subscript S indicates the value of G' and η at the reference temperature, T_S = 100°C.

Figure 9 Graph of log ($G\eta$) plotted against $\frac{1}{T\Delta T}$ for growth rates over the crystallization range.

Figure 10 The crystal growth rate, G cm/hr (corrected for viscosity (poises)) vs. the supercooling $\Delta T°$. Inset shows an enlarged view of the initial portion of the curve at small supercoolings.

Figure 11 Fluidity function $\log(\beta/\eta)$ vs. reduced temperature, τ, for molecular liquids. The points —●—●—●— are cis-decalin;[43] —◐—◐—◐— are o-terphenyl;[2,3] —□—□— are 1:3:5 triphenylbenzene;[45] and — ◔ — ◔ — ◔ — are TαNB. The solid line for "simple" liquids is from reference 42. The estimated fluidity[42] for a simple liquid at T_g is denoted by the solid point ▲, while T_g for TαNB and o-terphenyl[41] is indicated by an arrow.

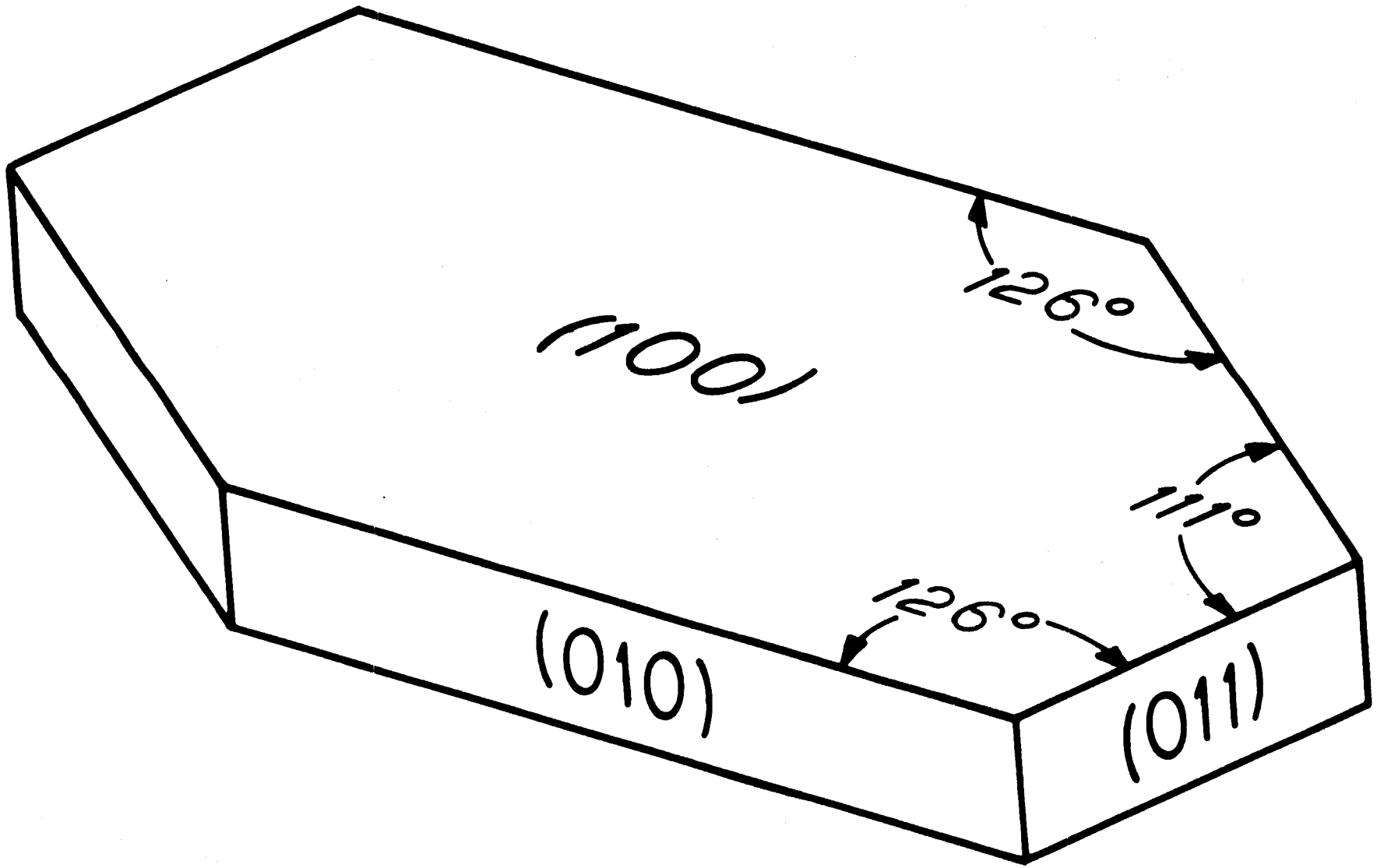

Figure 1

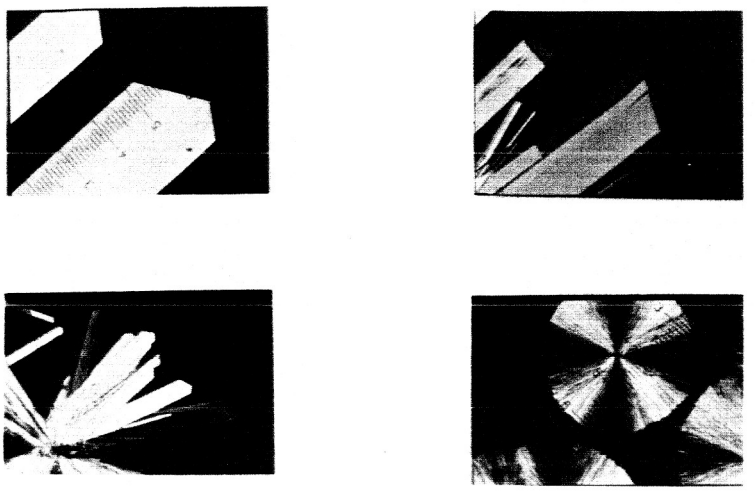

FIGURE 2

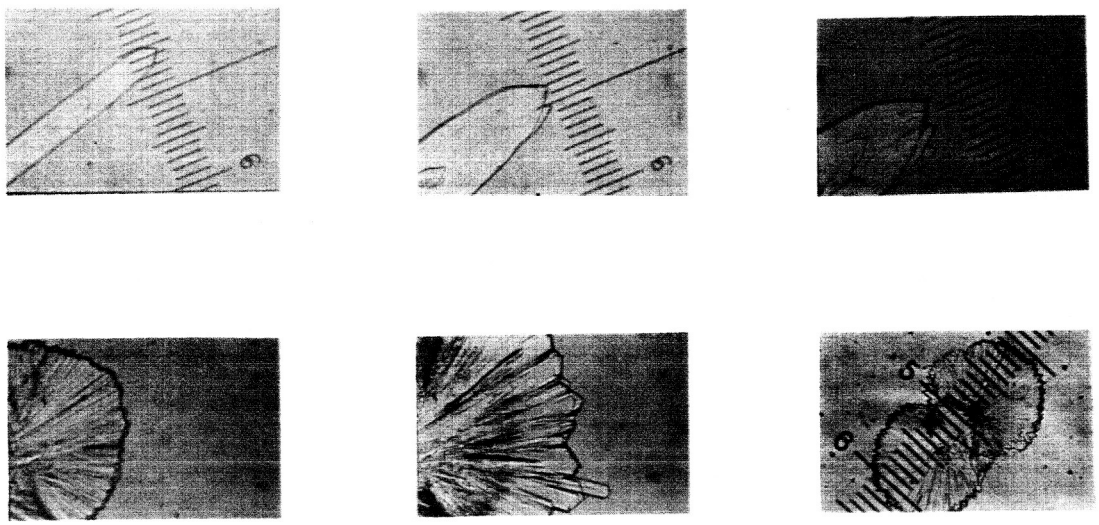

FIGURE 3

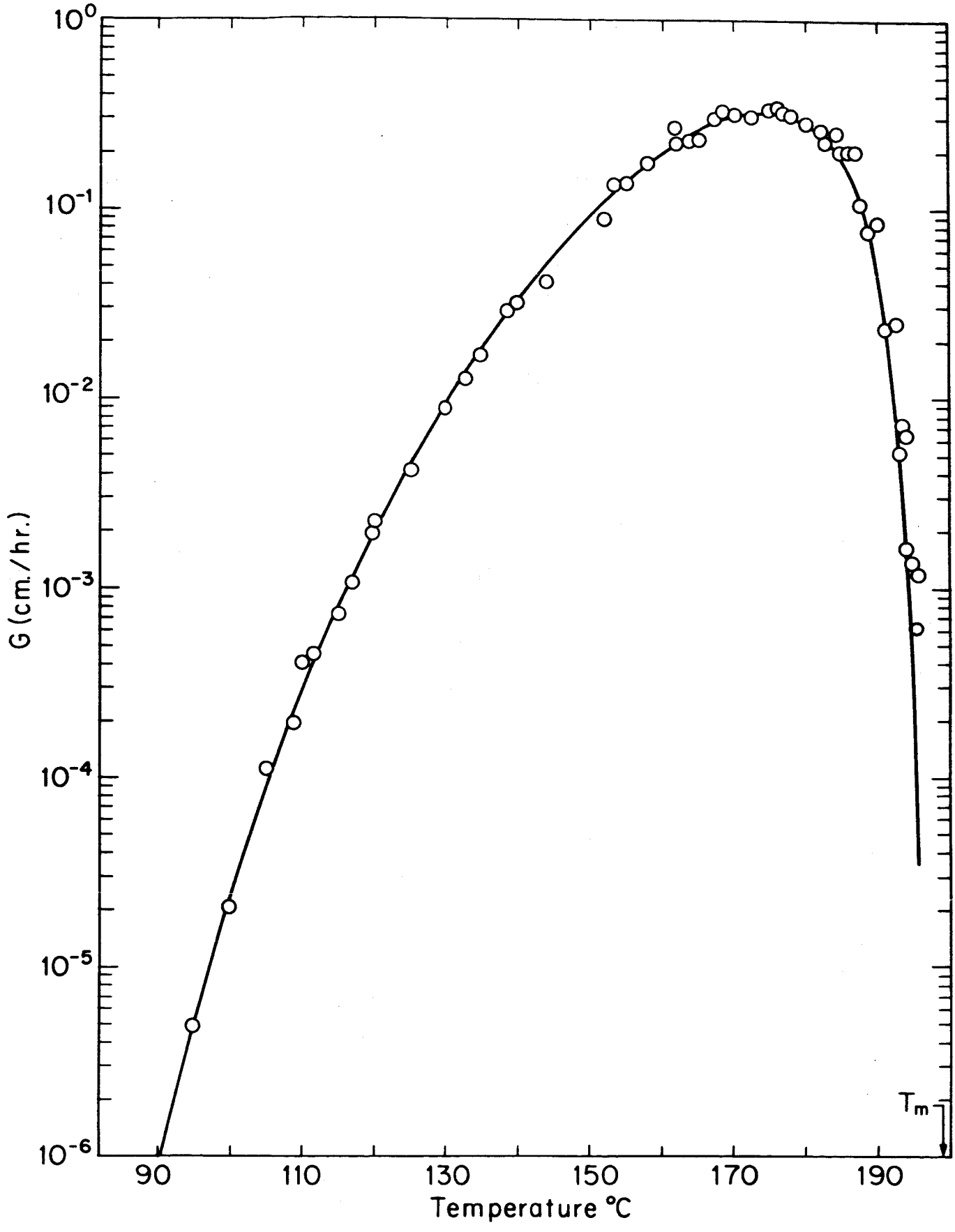
10^0
10^{-1}
10^{-2}
10^{-3}
10^{-4}
10^{-5}
10^{-6}
G (cm./hr.)
90
110
130
150
170
190
Temperature °C
T_m

Figure 4

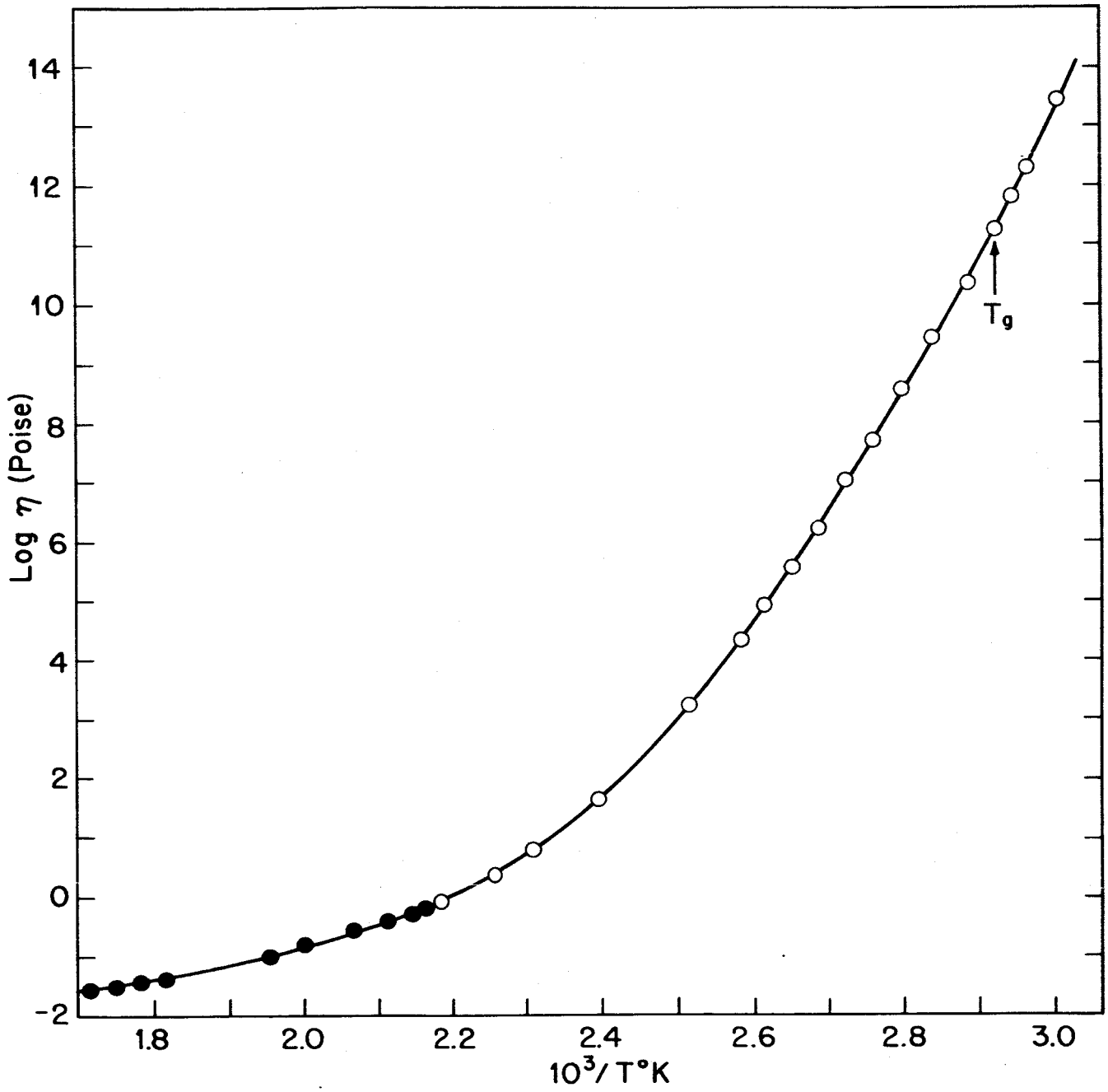

Figure 5

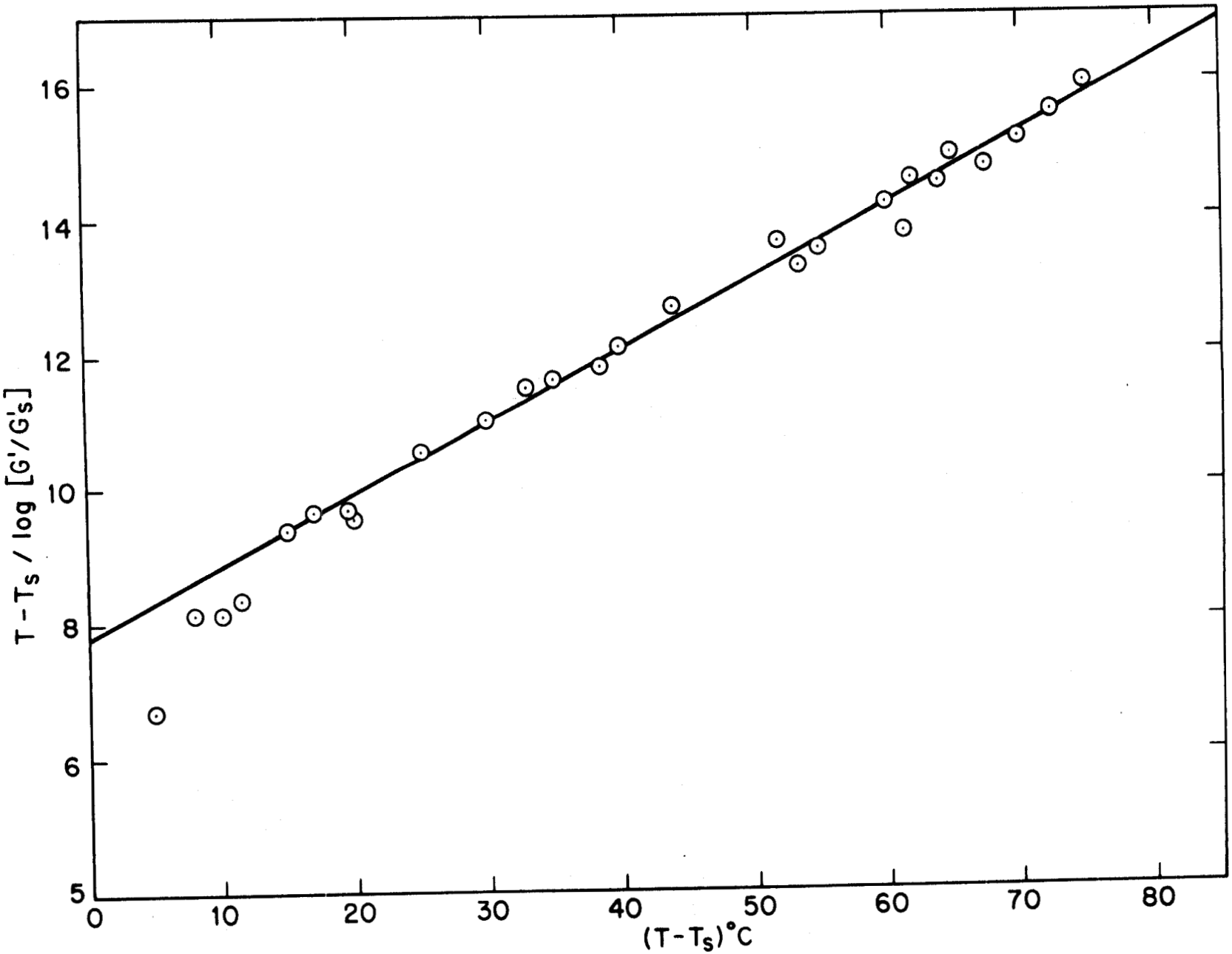

Figure 6

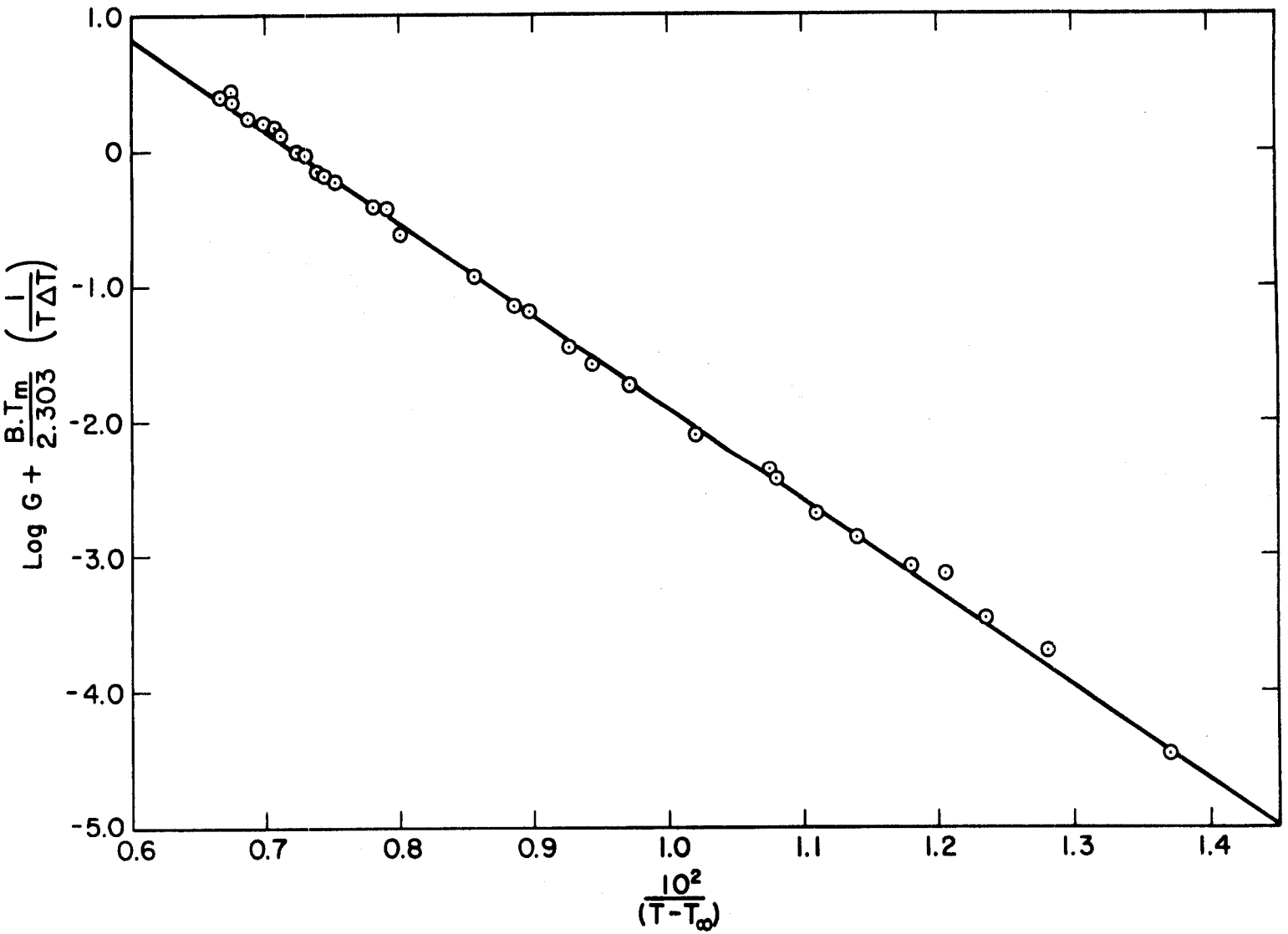
1.0
0
-1.0
-2.0
-3.0
-4.0
-5.0
0.6
0.7
0.8
0.9
1.0
1.1
1.2
1.3
1.4
Log G + B.Tm/2.303 (1/TΔT)
10²/(T-T∞)

Figure 7

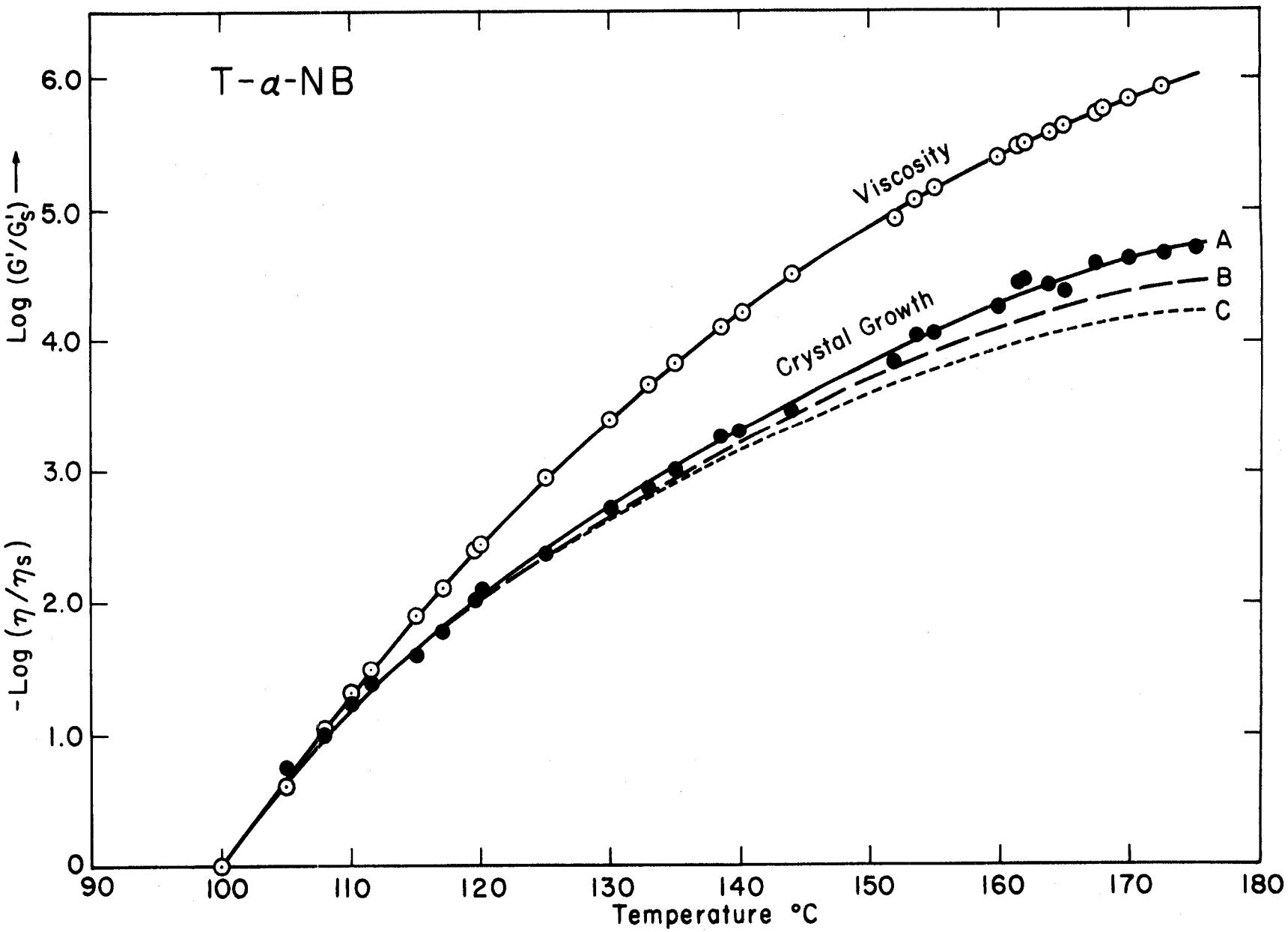
T-α-NB
Viscosity
Crystal Growth
A
B
C
Log (G'/G's) ⟶
-Log (η/ηs)
Temperature °C
6.0
5.0
4.0
3.0
2.0
1.0
0
90
100
110
120
130
140
150
160
170
180

Figure 8

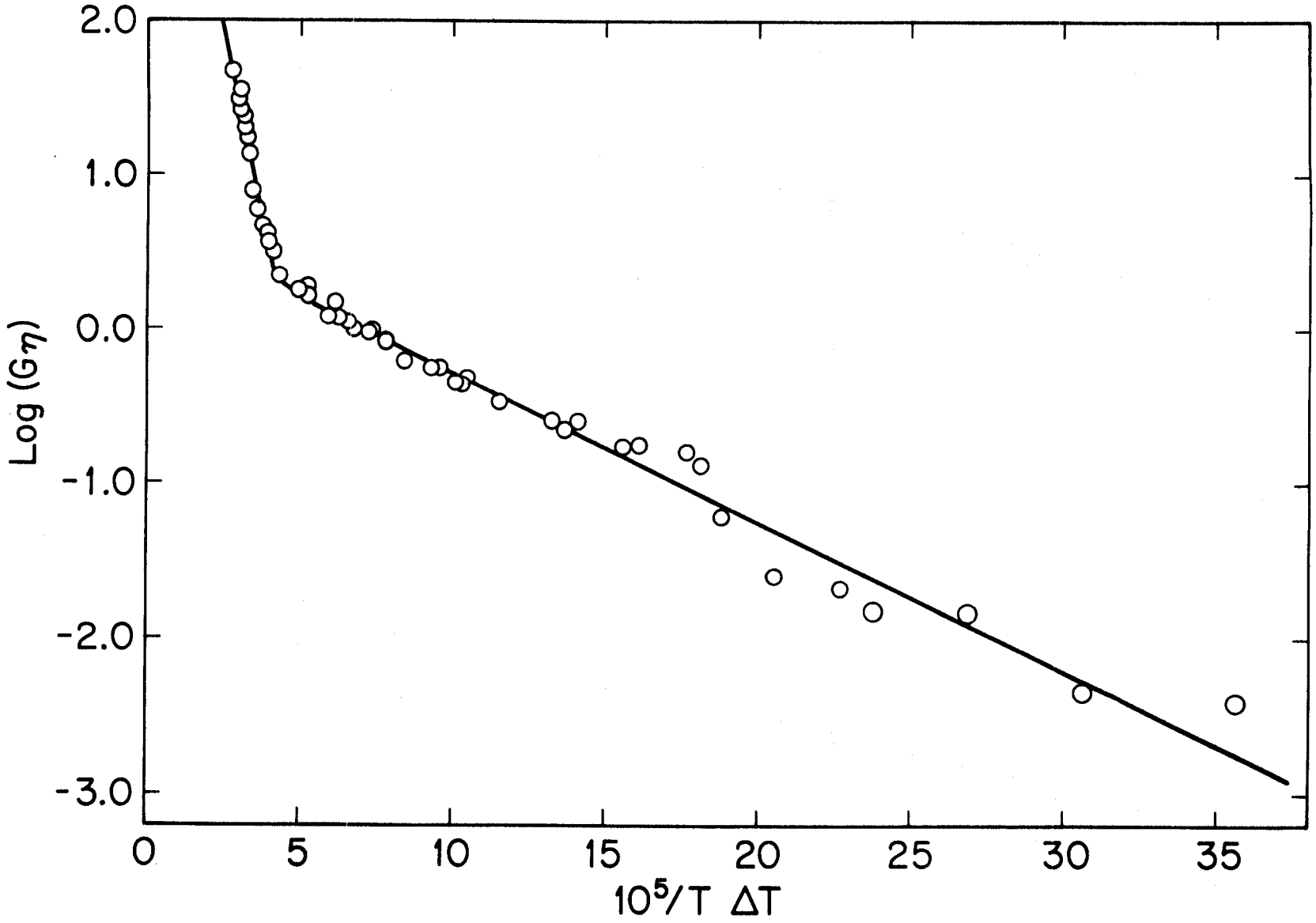

Figure 9

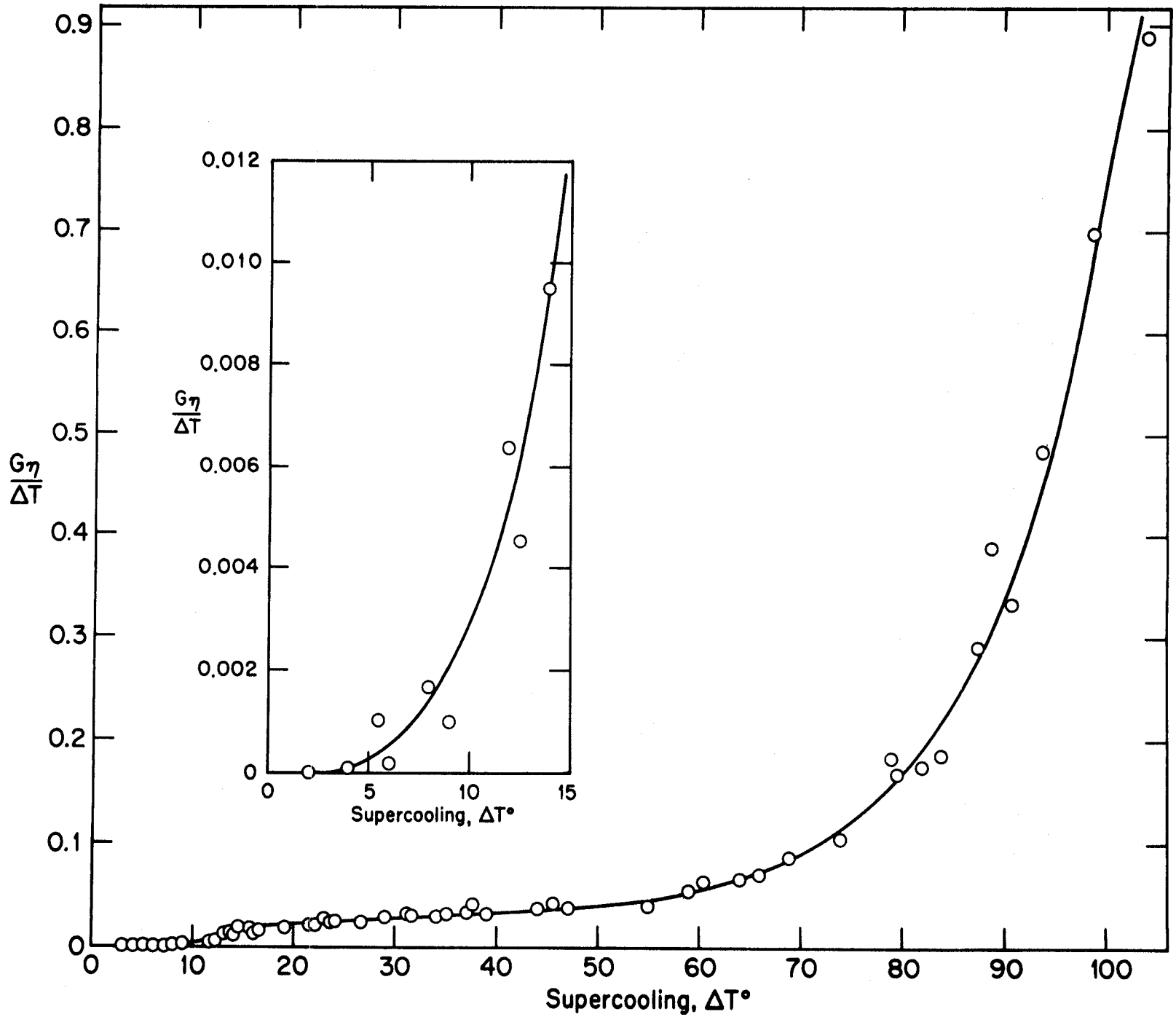
0.9
0.8
0.7
0.6
0.5
0.4
0.3
0.2
0.1
0
Gη/ΔT
0 10 20 30 40 50 60 70 80 90 100
Supercooling, ΔT°
0.012
0.010
0.008
0.006
0.004
0.002
0
Gη/ΔT
0 5 10 15
Supercooling, ΔT°

Figure 10

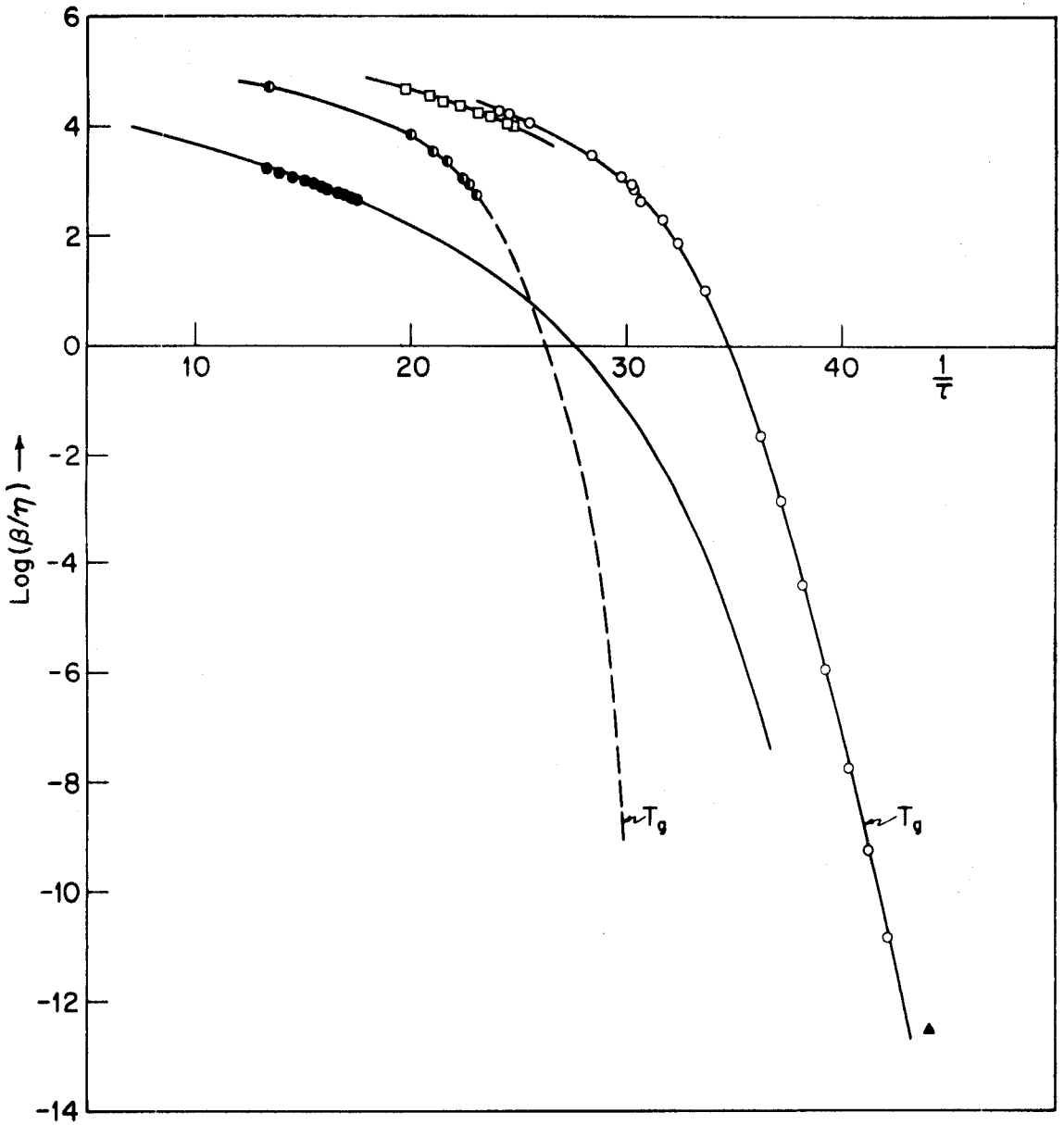

Figure 11